4-2009

Regulation of the mazEF Toxin-Antitoxin Module in Staphylococcus aureus and Its Impact on sigB Expression

Niles P. Donegan
Dartmouth College

Ambrose L. Cheung
Dartmouth College

JOURNAL OF BACTERIOLOGY, Apr. 2009, p. 2795–2805 Vol. 191, No. 8
0021-9193/09/$08.00+0 doi:10.1128/JB.01713-08

Regulation of the *mazEF* Toxin-Antitoxin Module in *Staphylococcus aureus* and Its Impact on *sigB* Expression[▽]

Niles P. Donegan and Ambrose L. Cheung*

Department of Microbiology and Immunology, Dartmouth Medical School, Hanover, New Hampshire 03755

Received 8 December 2008/Accepted 27 January 2009

In *Staphylococcus aureus*, the *sigB* operon codes for the alternative sigma factor σ^B and its regulators that enable the bacteria to rapidly respond to environmental stresses via redirection of transcriptional priorities. However, a full model of σ^B regulation in *S. aureus* has not yet emerged. Earlier data has suggested that *mazEF*, a toxin-antitoxin (TA) module immediately upstream of the *sigB* operon, was transcribed with the *sigB* operon. Here we demonstrate that the promoter P_{mazE} upstream of *mazEF* is essential for full σ^B activity and that instead of utilizing autorepression typical of TA systems, *sigB* downregulates this promoter, providing a negative-feedback loop for *sigB* to repress its own transcription. We have also found that the transcriptional regulator SarA binds and activates P_{mazE}. In addition, P_{mazE} was shown to respond to environmental and antibiotic stresses in a way that provides an additional layer of control over *sigB* expression. The antibiotic response also appears to occur in two other TA systems in *S. aureus*, indicating a shared mechanism of regulation.

The ability of the major human pathogen *Staphylococcus aureus* to respond to challenging biotic (e.g., the nares of healthy individuals) (27) and abiotic environments (e.g., catheters, clothing, and doorknobs) (45) has promoted its persistence and transmission within hosts. As a result, *S. aureus* is now endemic to many hospitals and has become the leading cause of postoperative surgical infections (46). Furthermore, these adaptive responses have contributed to the sharp increase in *S. aureus* skin and soft tissue infections seen in nonrisk populations in the community (26). The ability of *S. aureus* to survive adverse host conditions is mediated by the alternative sigma factor σ^B, which redirects RNA polymerase to transcribe genes involved in environmental stress responses (22). Although all σ^B-positive organisms use σ^B to regulate stress response, pathogenic organisms such as *S. aureus* and *L. monocytogenes* appear to have an expanded role for σ^B in virulence gene expression (5, 47). Therefore, determining how σ^B is regulated in *S. aureus* is crucial to understanding not only the bacteria's response to stress but also how it impacts virulence.

All σ^B-positive organisms appear to share a similar σ^B regulatory core, wherein σ^B is bound in an inactive state by its anti-sigma factor RsbW. Dephosphorylated RsbV, the anti-anti-sigma factor, disrupts the association of σ^B with RsbW, hence regulating the amount of free σ^B (24). However, regulation outside this core set of interactions is less well conserved among gram-positive bacteria. For example, *S. aureus* lacks equivalents to the physical stress sensing RsbRST and the nutritional state sensing RsbPQ of *Bacillus subtilis* (22). The only known regulator of the RsbV/RsbW interaction in *S. aureus* is RsbU, which promotes the disassociation of σ^B from RsbW by dephosphorylating RsbV. However, as σ^B is still partially active in a Δ*rsbU* mutant (36), additional factors are likely responsible for regulating this activity.

Immediately upstream of the *rsbUVW-sigB* operon, which codes for σ^B and its regulators, are two small genes, *mazF* (SA1873) and *mazE* (SAS0167) (see Fig. 1E), which similar to their *Escherichia coli* namesakes (1), encode a toxin-antitoxin (TA) system (17). TA systems are common among prokaryotes and typically consist of a labile antitoxin that binds and inactivates a more stable toxin (18). Cellular proteases (e.g., Lon and ClpP) normally degrade these antitoxins, ensuring toxin activation if antitoxin production ever becomes interrupted. Starvation and antibiotic exposure are the most well-described stimuli of TA systems, leading to hypotheses that TA systems could be used as either a form of bacterial programmed cell death or as a way to selectively shut down the bacterium's metabolism (1, 18). Other hypotheses have laid out possible roles of TA systems in stabilizing nearby sections of the chromosome, in phage resistance, or in mediating the emergence of persister cells (33).

In the present study, we expand the existing model of σ^B regulation in *S. aureus* to include the transcriptional contribution from P_{mazE}. We describe how the P_{mazE} impacts σ^B activity and how its activation by heat and antibiotic stress provides an additional mechanism for *sigB* regulation. We also detail the genetic regulation of this promoter, noting that transcriptional regulator SarA directly activates P_{mazE} and demonstrate that unlike other TA systems, the *mazEF* system is not autoregulated. Instead, this promoter is negatively regulated by *sigB*, which serves to create a feedback loop for repression of its own transcription. Together, these data allow us to update *S. aureus sigB* regulation, as well as to describe the genetic factors involved in the regulation of this TA system.

* Corresponding author. Mailing address: Department of Microbiology and Immunology, Dartmouth Medical School, Hanover, NH 03755. Phone: (603) 650-1310. Fax: (603) 650-1318. E-mail: ambrose.cheung@dartmouth.edu.

▽ Published ahead of print on 30 January 2009.

TABLE 1. Bacterial strains and plasmids used in this study

Strain or plasmid	Genotype and/or characteristics	Source or reference
Strains		
S. aureus		
RN4220	Heavily mutagenized NCTC 8325-4	28
Newman	Overexpresses *clfA* and *sae*	16
SA1873	Newman *mazF*::*mariner* at +6 of *mazF*	3
ALC1342	RN6390 *sarA*::*ermC*	9
ALC1820	Newman *sarA*::*ermC*, transductant of ALC1342	This study
ALC4072	Newman Δ*mazEF*	This study
ALC4434	Newman Δ*sigB*	This study
ALC4948	Newman P_{mazE} scramble	This study
ALC5084	Newman *mazEF* complement	This study
ALC5695	Newman *sigB* complement	This study
ALC5696	Newman *sarA* complement	This study
ALC6476	Newman Δ*axe1*/*txe1*	This study
ALC6477	Newman Δ*axe2*/*txe2*	This study
E. coli XL1-Blue	General purpose host strain for cloning	Agilent
Plasmids		
pCR2.1	Topo cloning vector	Invitrogen
pMAD	Allelic replacement vector	2
pALC1484	pSK236 containing promoterless gfp_{uvr} gene	10
pALC2201	pALC1484 with *asp23* promoter fragment	36
pALC3961	pALC1484 with P_{mazE} fragment	This study
pALC6478	pALC1484 with *axe1*/*txe1* promoter fragment	This study
pALC6479	pALC1484 with *axe2*/*txe2* promoter fragment	This study
pALC4401	pMAD/Δ*sigB*	This study
pALC4771	pMAD/*sigB* complement	This study
pALC4109	pMAD/Δ*mazEF*	This study
pALC4772	pMAD/*mazEF* complement	This study
pALC5708	pMAD/P_{mazE} scramble	This study
pALC5699	pMAD/*sarA* complement	This study
pALC6480	pMAD/Δ*axe1*/*txe1*	This study
pALC6481	pMAD/Δ*axe2*/*txe2*	This study

MATERIALS AND METHODS

Bacterial strains, plasmids, primers, and growth conditions. All bacterial strains and plasmids used in the present study are listed in Table 1. Unless otherwise noted, cells were grown shaking at 250 rpm at 37°C in Luria-Bertani (LB) for *E. coli* or Trypticase soy broth (TSB; Fisher Scientific) or 03GL for *S. aureus* strains. Optical densities were recorded by their measurement in a Biotek FL600 (BioTek Instruments) or by dilution of cultures to the linear range of a Spectronic 20D+ (Spectronic). Antibiotics were used at the following concentrations: erythromycin at 2.5 μg/ml, ampicillin at 50 μg/ml, and chloramphenicol at 10 μg/ml. The sequences of oligonucleotides used (IDT Technologies) are available upon request.

Genetic manipulations. Plasmids were isolated from *E. coli* using the Qiaprep Spin Kit (Qiagen), and from *S. aureus* as described previously (42). Transduction of the *sarA*::*ermC* disruption from ALC1342 to Newman was carried out using phage 80α as described previously (44).

***gfp*$_{uvr}$ reporter gene constructs.** Transcriptional gfp_{uvr} fusions to various promoters were created by cloning PCR-amplified promoter fragments from strain Newman into pCR2.1 using the Topo TA cloning kit (Invitrogen). Recombinant pCR2.1 plasmids were digested with EcoRI and the promoter fragment subcloned into pALC1484, a shuttle plasmid containing a promoterless gfp_{uvr}. Ligation products were verified by restriction digestion and sequenced for correct orientation.

Allelic replacement and complementation in *S. aureus*. Flanking sequences ~1 kb on either side of the gene to be deleted were amplified by PCR from the Newman chromosome, joined together via complementary overhangs and reamplified by using a second set of flanking primers in a subsequent PCR. The resulting ~2-kb PCR product was then ligated into pMAD, a temperature-sensitive shuttle plasmid. Allelic exchange was then performed as described previously (2). To create an *S. aureus* strain with altered σ^A binding sites at the P_{mazE}, complementary primers containing G/T and A/C transversions at the −10 and −35 promoter boxes upstream of *mazE* (SAS0167) were used to perform site-directed mutagenesis with the QuikChange II kit (Agilent) on pALC4772, a derivative of pMAD containing the native *mazEF* genes. Transversions at both sites were verified by sequencing, and this plasmid containing the mutated P_{mazE}, as well as an intact copy of *mazEF*, was used in allelic replacement in ALC4072, a *mazEF* deletion mutant of Newman. To complement these deletions and mutations, a pMAD construct containing the target gene flanked by ~1 kb on either side was used to return the gene to the chromosome by using allelic replacement. All generated strains were verified by PCR and chromosomal sequencing.

Gel shift analysis. Electrophoretic mobility shift assays (EMSA) were performed with purified MazE (17), MazF (17), or SarA (a gift from Gongyi Zhang, National Jewish Hospital) using promoter fragments end labeled with [γ-^{32}P]ATP by T4 polynucleotide kinase (NEB) and purified by ProbeQuant G-50 microcolumns (GE) according to the manufacturer's instructions. The labeled DNA fragment (1.8 nM; 10,000 cpm) was incubated at room temperature for 20 min with the indicated amounts of purified protein in 25 μl of binding buffer (25 mM Tris-HCl [pH 7.5], 0.1 mM EDTA, 75 mM NaCl, 1 mM dithiothreitol and 5% glycerol) containing 0.5 μg of calf thymus DNA. Samples were then resolved on 6% polyacrylamide gels in 0.5× Tris-borate-EDTA, dried, and autoradiographed.

Quantitation of *sigB* phenotypes. Staphyloxanthin production in various strains was quantitated as described earlier (30). Spontaneous and induced autolysis assays were performed as described previously (29).

Isolation of RNA and Northern blot hybridization. Overnight cultures of *S. aureus* were diluted 1:1,000 in 100 ml of TSB in 250 ml side-arm flasks (flask/medium ratio of 2.5:1) and grown shaking at 250 rpm at 37°C. The cells were withdrawn at various time points and centrifuged at 4°C for 10 min, and the pellets were frozen in liquid nitrogen until all samples from all time points were collected. The cells were then disrupted with 1 ml of cold TRIzol (Invitrogen) plus 0.25 ml of 0.1-mm-diameter silica/glass beads (Biospec Products) in a reciprocating shaker at the maximum setting for two 1-min pulses (Biospec Products). RNA purification and subsequent Northern analysis was then performed as described previously (8).

Quantification of transcript levels by real-time PCR. RNA was isolated as described above except that purified RNA was resuspended in diethyl pyrocarbonate-treated double-distilled water. Real-time PCR was conducted as described previously (34), and quantification of the cDNA levels relative to *gyrB* was performed according to the instructions of the Maxima SYBR kit (Fermentas) with a LightCycler 1.5 system (Roche). Relative quantification analysis was done using the LightCycler software version 4.0 (Roche).

Primer extension analysis. Mapping the 5′ end of the *mazEF* transcript by primer extension was performed using two primers complementary to the *mazEF* coding strand located at either nucleotide position +146 or +74 from the ATG start codon. Primer extension was carried out by using 30 μg of total RNA isolated from Newman wild type grown to postexponential phase as described previously (4). The same radiolabeled primer was used for DNA sequencing reactions to provide the reading frame.

Transcriptional fusion analyses. Overnight cultures of *S. aureus* strains containing transcriptional fusions of various promoters to gfp_{uvr} were diluted to an A_{650} of 0.1 in TSB containing 10 μg of chloramphenicol/ml and grown at 37°C with shaking (250 rpm) (tube/medium ratio of 6:1). Aliquots were then taken at various time points, whereupon the fluorescence and A_{650} were measured by using a FL600 microplate reader. For solid medium assays, 50 μl of an overnight culture was spread on Trypticase soy agar containing 10 μg of chloramphenicol/ml and incubated at 37°C for 24 h with an antibiotic disk (BD) or an Etest strip (AB Biodisk). Fluorescence was then recorded by a digital camera using a 485-nm light source and a 518-nm filter. To isolate RNA, the ~2-mm region proximal to the growth-inhibitory ring created by diffused antibiotics were scraped and resuspended into sterile phosphate-buffered saline. RNA was extracted immediately from half of these cells as described above, while the remaining half were evaluated for fluorescence and A_{650} in a Biotek FL600 microplate reader.

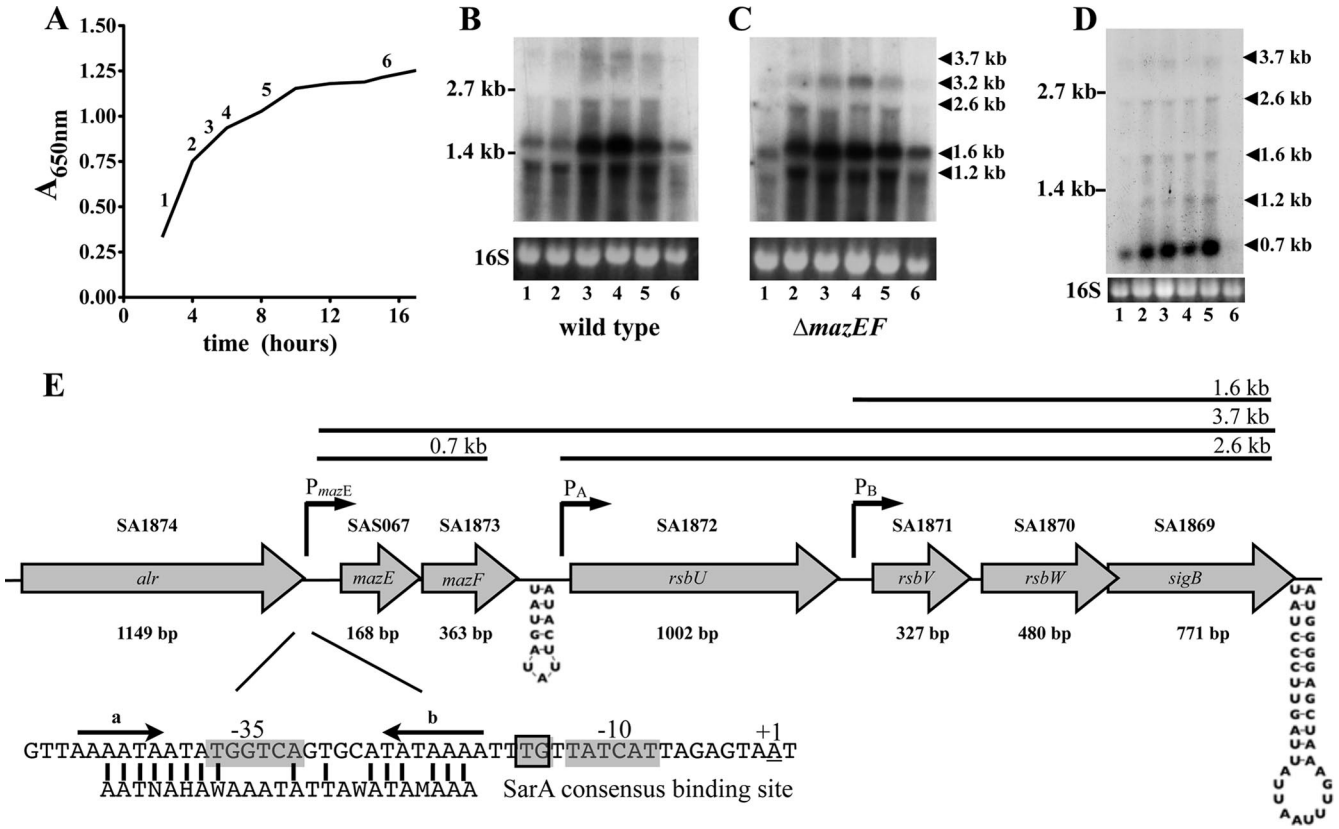

FIG. 1. Analysis of *mazEF* and *sigB* operon transcription. (A) Samples were withdrawn at various points during growth (indicated as points 1 to 6), and their A_{650} values were measured by using a Biotek FL600. (B to D) Northern blot analysis of these time points showing *sigB* transcripts from Newman wild-type (B) and Δ*mazEF* (C) strains and of *mazF* transcripts from Newman wild type (D). The sizes of relevant bands are indicated on the right, and rRNA sizes are indicated to the left. Ethidium bromide staining of 16S rRNA is shown to demonstrate equivalent RNA loading. (E) Schematic model of the *mazEF* and *sigB* operons in *S. aureus*. Transcripts and their respective promoters are above the diagram, while *rho*-independent transcriptional terminators are indicated below. The $-\Delta G$ values for the terminators downstream of *mazF* and *sigB* are 3.6 and 16.9 kcal/mol, respectively. Locus names and their respective lengths are from the N315 genome annotation. Shown in detail is the promoter P_{mazE}, with its predicted transcriptional start site (+1, underlined), −10 and −35 σ^A binding sites (highlighted in gray), and TG residues indicating an extended −10 region (gray highlight with black border). Arrows a and b mark an inverted repeat of DNA and the SarA consensus binding site (12), and the homology to the P_{mazE} region is indicated at the bottom.

RESULTS

***mazEF* is transcribed both as part of the *sigB* operon and as a smaller transcript.** The *mazEF* genes encode a TA system (17) located immediately upstream of the *rsbUVW-sigB* operon and have been reported to be transcriptionally linked during heat shock (19, 29, 43). However, the transcriptional profile of these genes outside of heat shock has not been well characterized. Accordingly, we examined their transcription during various stages of cell growth. Northern blot analyses using a *sigB* probe were performed on RNA isolated from Newman wild type at various points during exponential and stationary growth (Fig. 1A). *sigB*-containing transcripts 3.7, 2.7, 1.6, and 1.2 kb in size were seen in growth phases from early exponential through early-stationary-phase cultures when grown either in TSB (Fig. 1B) or 03GL (data not shown). However, during late-stationary-phase conditions (t = 16 h, Fig. 1A), *sigB*-related transcription was markedly decreased, most notably the 3.7-kb transcript. To identify whether this 3.7-kb *sigB* transcript also contained *mazEF*, we isolated RNA from a Δ*mazEF* strain grown to similar time points in TSB. As seen from comparing Fig. 1B and C, the 3.7-kb band seen in wild type was replaced by a 3.2-kb band in the Δ*mazEF* strain, a size difference that corresponded to the deletion of *mazEF* (530 bp). These data implied that *mazEF* was transcriptionally linked to the *sigB* operon during normal growth conditions and that, as a culture enters the late stationary phase, the transcription of *sigB* and *mazEF* both become greatly reduced.

In order to fully characterize the transcriptional activity of this locus, a *mazF* probe was also hybridized to wild-type Newman RNA. As expected, the 3.7-kb transcript was present at a low level throughout growth until it disappeared in late stationary phase (t = 16 h) (Fig. 1B). To confirm that the 3.7-kb transcript indeed encompassed *mazEF*, as well as the *sigB* operon (*rsbUVW-sigB*), we created a Newman strain with its *mazEF* genes intact but with an inactivated promoter. To identify the exact site of P_{mazE}, we performed primer extension studies on mRNA isolated from strain Newman. In agreement with data from Senn et al. (43), the transcriptional start site was found to be 46 bp upstream of the translational start site of *mazE* (data not shown), and the deduced −10 and −35

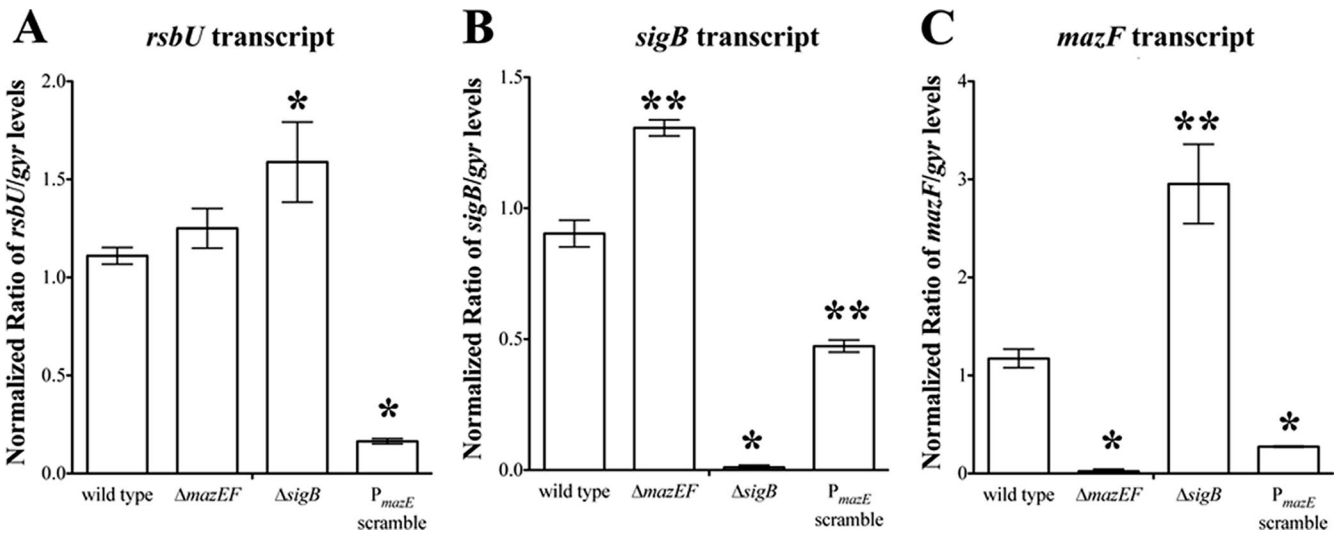

FIG. 2. Real-time PCR analysis of transcripts in the *mazEF-rsbUVW-sigB* operon. Relative quantification analyses of cDNAs derived from RNA of late-logarithmic-phase (A_{650} = 1.5) *S. aureus* cells were made using primer pairs to *rsbU* (A), *sigB* (B), or *mazF* (C) and normalized to *gyrB* levels. The data represent mean values for three experiments ± the standard deviation. *, $P < 0.0001$; **, $P \leq 0.0003$ (compared to the control [Student *t* test]).

promoter boxes were found to be consistent with those of a σ^A-regulated promoter. We also noted the presence of a 5′-TG-3′ site at position −15/−16 (shaded box in Fig. 1E). This suggests that P_{mazE} has an extended −10 motif, which provides additional points of contact for the RNA polymerase holoenzyme (7, 23). Based on this information, we created a P_{mazE} scrambled strain with transversional mutations in these −10 and −35 regions (unboxed shaded regions in Fig. 1E). Northern blot analysis of this strain using a *sigB* probe confirmed the absence of the 3.7-kb transcript but not of the 2.6- and 1.6-kb transcripts (data not shown).

To ascertain whether inactivation of P_{mazE} or deletion of the *mazEF* genes affected expression of *rsbU*-related transcripts, we conducted real-time PCR with *rsbU* specific primers. Interestingly, *rsbU*-related transcripts remained unchanged in the Δ*mazEF* mutant compared to the wild type, suggesting that the *mazEF* genes do not themselves modulate the activity of P_A, the σ^A-dependent promoter immediately upstream of *rsbU* (Fig. 1E). In contrast, *rsbU*-related transcripts were markedly decreased in the P_{mazE} scramble strain (Fig. 2A), demonstrating that the 3.7-kb *mazEF-rsbUVW-sigB* transcript from P_{mazE} contributes significantly to *rsbU*-related transcription and that the P_A promoter that initiates the *rsbUVW-sigB* transcript is likely to be weak.

Besides the 3.7-kb transcript, several smaller transcripts also appeared in the *mazF* Northern blot (Fig. 1D). While most of these are likely cross-hybridization bands generated from high amounts of nearby 23S and 16S rRNA, a distinct ~700-bp transcript was observed, a size that corresponds to *mazEF* (530 bp) (Fig. 1D). These data indicated that *mazEF* was not only part of the *sigB* operon but was also transcribed as a smaller transcript on its own. Furthermore, this transcript was shown to be lacking in both the P_{mazE} scramble strain and the Δ*mazEF* strain (data not shown). The existence of the 0.7-kb transcript prompted us to look for some form of transcriptional termination downstream of *mazF*. In silico work by de Hoon et al. (14) has previously predicted a *rho*-independent terminator 184 bp after the *mazF* stop codon (Fig. 1E). However, the free energy for this stem-loop is very low compared to the average free energy of hairpin structures in *S. aureus* ($-\Delta G$ = 3.6 versus 16.9 kcal/mol, respectively) (14), thus suggesting that transcriptional readthrough could occur to yield both the 0.7- and 3.7-kb *mazEF*-related transcripts.

P_{mazE}, but not *mazEF*, is necessary for full σ^B activity. An early observation spurring our interest in *mazEF* was that the activity of the *sigB*-dependent *asp23* promoter was greatly reduced in a *S. aureus* Newman strain containing a *mariner* transposon insertion in *mazF* (data not shown). When we evaluated a Newman strain with a clean deletion of the *mazEF* genes (ALC4072) in a similar manner, no difference in either *asp23* promoter activity was observed between this mutant and its parent, however, (Fig. 3A). A slight increase in *sigB* transcription was seen in this strain by real-time PCR analysis (Fig. 2B) but not at a level detectable by Northern analysis (Fig. 1B and C). As an additional verification that *mazEF* did not affect σ^B activity, the *sigB*-dependent P_B was also shown not to be altered in a Δ*mazEF* strain when examined with a transcriptional fusion of P_B to gfp_{uvr} (data not shown).

We next considered the possibility that P_{mazE} itself may contribute to σ^B activity since the *mazF*::*mariner* insertion might have also disrupted this upstream promoter. In comparing the *asp23* promoter activity of the P_{mazE} scramble to that of the wild type, we found greatly reduced but not abolished activity in the promoter scramble strain (Fig. 3A), similar to the levels seen in the *mazF*::*mariner* strain. We also ascertained the level of *sigB* transcript in this promoter scramble strain by real-time PCR and found it to be intermediate between the wild type and the Δ*sigB* mutant (Fig. 2B). These data linked the reduction in overall σ^B activity to the alterations in the −10 and −35 promoter boxes of P_{mazE}, thus indicating P_{mazE} contributes to optimal transcriptional activation of *sigB*.

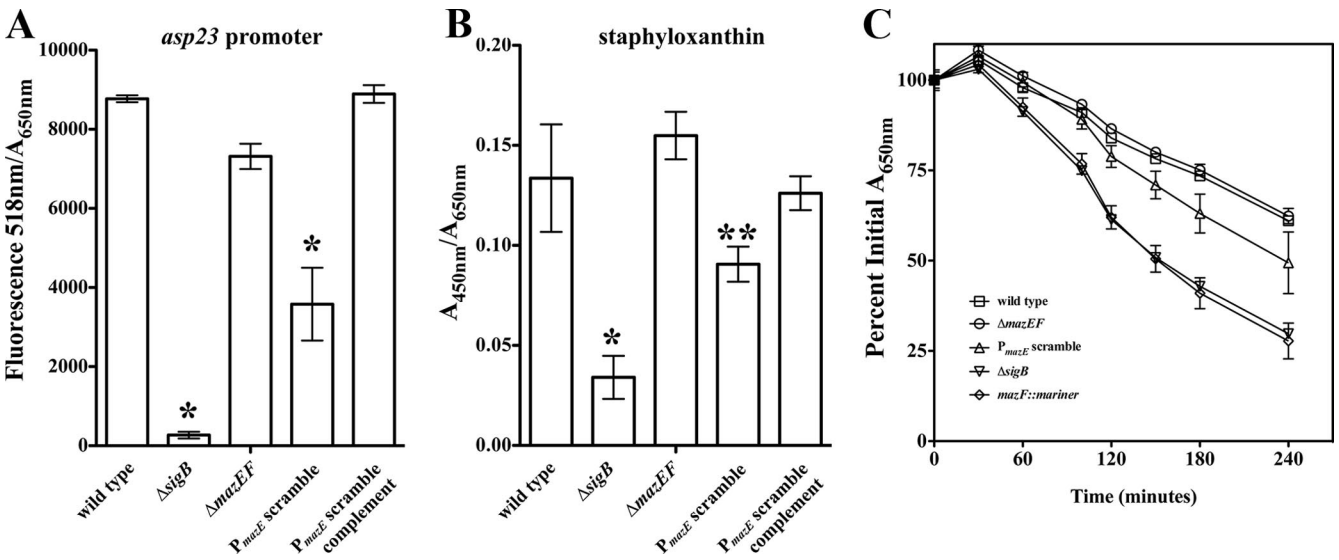

FIG. 3. Quantitation of *sigB* phenotypes. (A) Overnight (16 h) fluorescence levels (518 nm) from strains containing pALC2201, a plasmid with *asp23* promoter fusion to gfp_{uvr}, were recorded and normalized to A_{650}. (B) Methanol-extracted staphyloxanthin levels were determined by A_{450} and normalized to the cell number (A_{650}). (C) Rates of induced autolysis in 0.05% Triton X-100 static at 30°C were measured by comparing the A_{650} of each strain at time points as a percentage of their original A_{650}. Symbols: □, wild type; ○, ΔmazEF; △, P_{mazE} scramble; ▽, Δ*sigB*; ◇, *mazF*::*mariner*. The data represent mean values for three experiments ± the standard deviation. *, $P \leq 0.005$; **, $P \leq 0.05$ (compared to the control [Student *t* test]).

Inactivation of P_{mazE} results in partial *sigB* deficient phenotypes. Since transversional mutations in P_{mazE} resulted in decreased σ^B activity, we investigated whether this strain exhibited other *sigB*-deficient phenotypes. Since the *S. aureus* pigment staphyloxanthin has been demonstrated to be regulated by *sigB* (25), we quantitated staphyloxanthin levels for wild-type, Δ*sigB*, Δ*mazEF*, and P_{mazE} scramble strains. As seen in Fig. 3B, the staphyloxanthin level of a Δ*mazEF* strain was unchanged relative to wild type, while it was reduced in a P_{mazE} scramble strain. As a control, the Δ*sigB* mutant exhibited a very low level of staphyloxanthin pigment. Notably, the pigment level in the promoter scramble strain was not as low as that of the Δ*sigB* strain, thus indicating partial σ^B activity, consistent with the pattern that we have observed with regard to *asp23* promoter activity levels.

We also examined autolysis in these strains because (i) Kullik et al. noted an autolysis defect in IKA54, a *S. aureus* 8325-4 strain with an integrated plasmid disrupting the 1.1-kb region of *alr* and *mazE* (29), and (ii) autolysis is negatively regulated by *arlRS*, which in turn is positively controlled by *sigB* (35). While rates of spontaneous autolysis were found to be unchanged in these strains (data not shown), significant differences were seen when cells were exposed to 0.05% Triton X-100, an autolysis-inducing condition (Fig. 3C). Both the

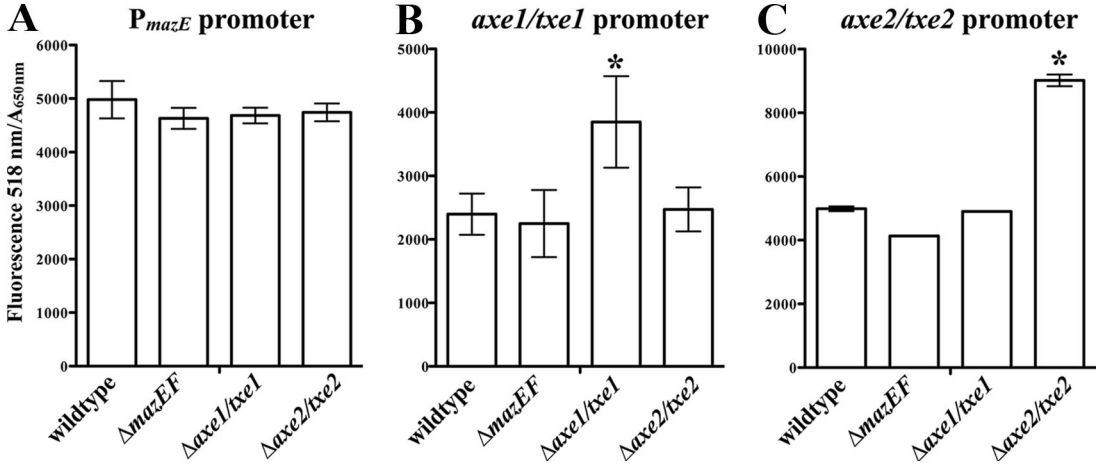

FIG. 4. TA promoter levels in *S. aureus* wild-type and TA deletion strains. Strains transformed with plasmids containing transcriptional fusions to gfp_{uv} under the control of P_{mazE} (pALC3961) (A), *axe1*/*txe1* promoter (pALC6478) (B) or *axe2*/*txe2* promoter (pALC6479) (C) were grown overnight (16 h), and their fluorescence levels at 518 nm were measured and normalized to the A_{650}. The data represent mean values for three experiments ± the standard deviation. *, $P < 0.05$ (compared to the control [Student *t* test]).

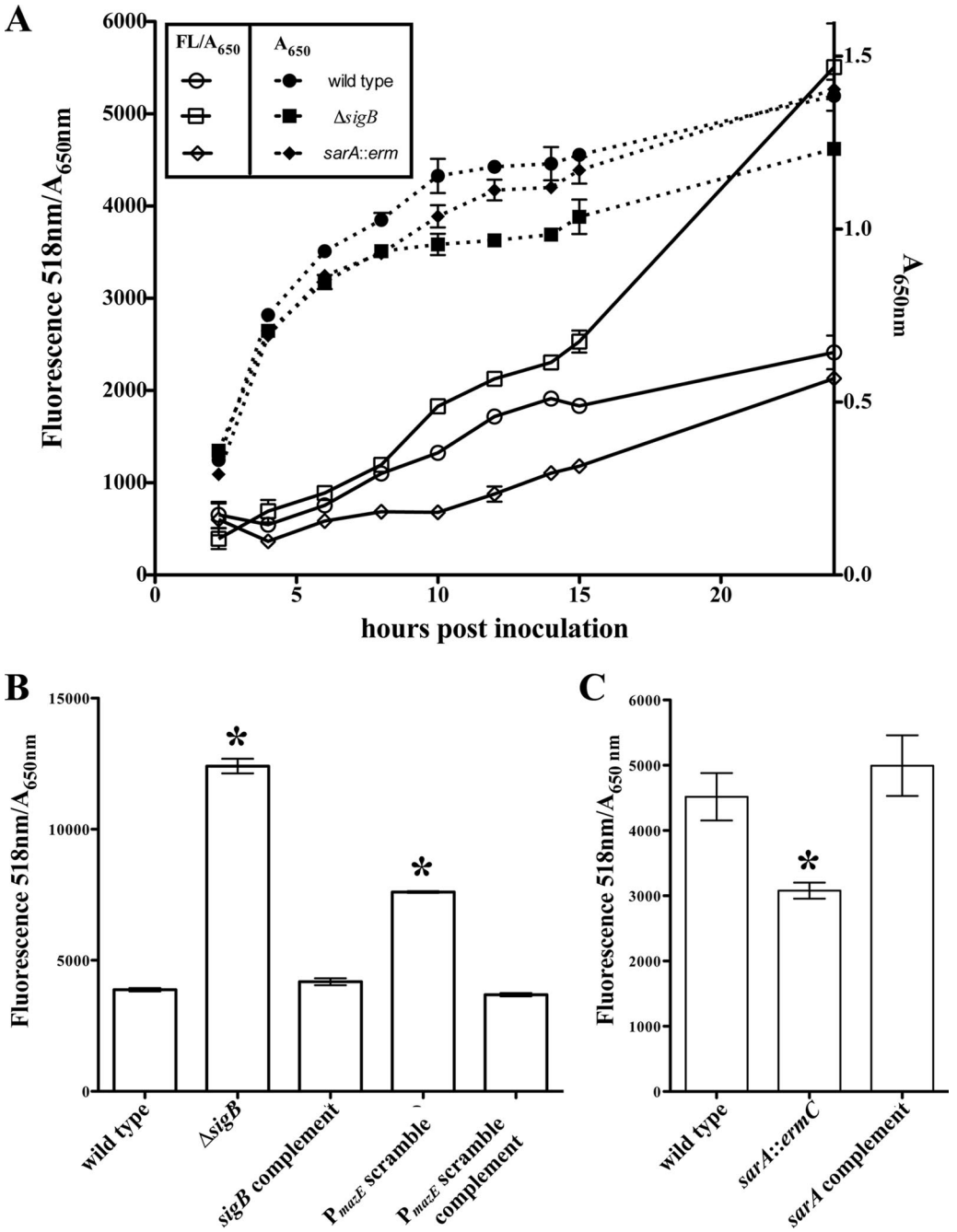

FIG. 5. Effect of *sarA* and *sigB* on the promoter P_{mazE}. (A) Fluorescence (518 nm) levels were normalized to the A_{650} of Newman wild-type, sarA::*ermC* and Δ*sigB* strains carrying a transcriptional fusion of P_{mazE} to gfp_{uvr} (pALC3961) during growth through 24 h. (B and C) Fluorescence at 518 nm from wild-type, Δ*sigB*, *sarA*::*ermC*, and P_{mazE} scramble strains and their complementation strains. The data are presented as mean values for three experiments ± the standard deviation. *, $P < 0.0001$ (compared to the control [Student *t* test]).

Δ*sigB* mutant and the *mazF*::*mariner* mutant (tested for its similarities to IKA54) showed significantly enhanced autolytic activities compared to the wild-type or Δ*mazEF* strains, but the P_{mazE} scramble strain had an autolysis phenotype intermediate between the wild-type and the Δ*sigB* strains. These findings supported our hypothesis of reduced σ^B activity in the P_{mazE} scramble strain and indicated that transcription from P_{mazE} is necessary for full expression of *sigB*.

P_{mazE} in *S. aureus* is not autoregulated. A common mechanism of regulation among TA systems is that the antitoxin, either with or without its cognate toxin, binds at specific palindromic sequences and hence represses its own promoter (20, 48). However, no such motifs were found in the *S. aureus* P_{mazE} promoter using in silico analyses; curiously, a region of inverted repeats at −19 to −45 bp upstream of the transcriptional start site was found (arrows in Fig. 1E). To address

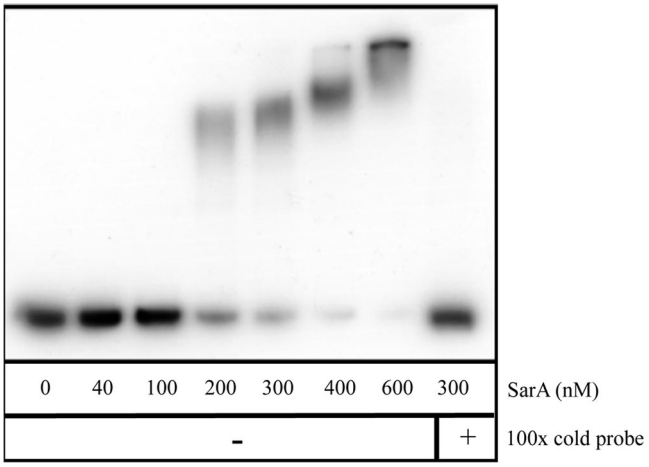

FIG. 6. SarA EMSA using a P_{mazE} fragment. A [γ-^{32}P]ATP-labeled P_{mazE} fragment (1.8 nM; positions −12 to −150 bp from the *mazE* start codon) was incubated with increasing concentrations of SarA protein (nM) and resolved by native polyacrylamide gel electrophoresis. Specific competition for P_{mazE} by SarA was performed by the addition of 100-fold excess unlabeled P_{mazE}.

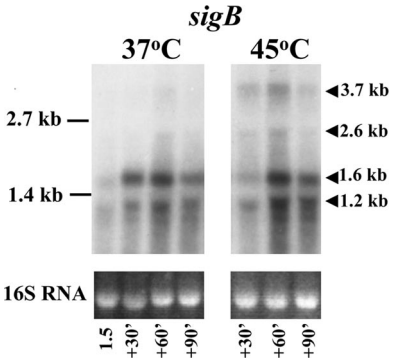

FIG. 7. Northern blot analysis of *sigB* transcripts from Newman wild type during growth at 37°C or after a shift to 45°C. The sizes of the relevant bands are indicated on the right, and rRNA sizes are indicated to the left. Ethidium bromide staining of 16S rRNA is shown to demonstrate equivalent RNA loading.

whether MazE and/or MazF interacted with this or another cryptic binding site, we performed electrophoretic mobility shift assays (EMSAs) with a P_{mazE} fragment spanning −12 to −150 bp upstream of the *mazE* start codon and purified MazE and/or MazF (17) at concentrations ranging from 40 to 960 nM (48). However, these studies failed to disclose an interaction between MazE and/or MazF and the promoter fragment (data not shown). Additional EMSAs using the promoters upstream of *rsbU* and *rsbV* and MazE and/or MazF also did not show any binding activity (data not shown). To confirm this lack of association for P_{mazE}, we examined P_{mazE} activity in both Newman wild-type and Δ*mazEF* mutant strains containing a *mazEF* transcriptional fusion to gfp_{uvr} *in trans* (pALC3961). As comparisons, we also constructed strains with deletions of two other TA systems, *axe1*/*txe1* and *axe2*/*txe2* (SA2196-5 and SA2246-5, respectively) (21, 38), and transformed these strains with plasmids containing TA promoters driving gfp_{uvr} transcriptional fusions. While both *axe1*/*txe1* and *axe2*/*txe2* showed specific repression of their own promoters (Fig. 4B and C), similar autorepression did not exist for the *mazEF* system (Fig. 4A). Collectively, these data suggest that *mazEF* is unique among *S. aureus* TA systems in that it does not repress its own promoter.

P_{mazE} is negatively regulated by *sigB*. Since *mazEF* lacked a form of regulation conserved among all other TA systems (17), we screened a variety of *S. aureus* mutant strains containing pALC3961, a plasmid containing P_{mazE} driving gfp_{uvr}, for possible regulators of P_{mazE}. Interestingly, we observed increased fluorescence in a *sigB* deletion mutant compared to the wild type (Fig. 5A), up to a threefold increase after overnight growth (Fig. 5C). This increase returned to wild-type levels upon complementation (Fig. 5B). This repression on P_{mazE} by *sigB* was also corroborated by other studies, including (i) real-time PCR data showing both increased *mazF* and *rsbU* transcripts in a Δ*sigB* mutant strain compared to the Newman wild type (Fig. 2A and C); (ii) increased *mazEF* transcription rates in strains with mutations in positive regulators of σ^B activity (e.g., *rsbU* and *rsbV* mutants) (data not shown); (iii) the *rsbU*-deficient strain RN6390 had increased *mazEF* transcription compared to the *rsbU*-restored strain SH1000 (data not shown); and (iv) the P_{mazE} scramble mutant, which exhibited decreased σ^B activity, showed enhanced *in trans mazEF* transcriptional activity from pALC3961 compared to the wild type (Fig. 5B). Taken together, these data indicate that *sigB* represses *mazEF* transcription.

P_{mazE} is positively and directly regulated by *sarA*. Our screen for *S. aureus* strains with mutations affecting P_{mazE} activity also showed that a *sarA*::*ermC* mutant had decreased P_{mazE} activity compared to wild type during growth (Fig. 5A), although this difference was narrowed somewhat in overnight growth (Fig. 5C). The decrease in P_{mazE} activity in the *sarA* mutant was restored to the wild-type level upon complementation (Fig. 5C). As *sarA* is a global regulator in *S. aureus* at the center of a complex network of gene regulation (11, 15), it was necessary to ascertain whether SarA interacted directly with P_{mazE}. Interestingly, a region of high homology to the consensus SarA binding site (12) containing an imperfect 8-bp palindromic sequence (AAAATATA) flanked by a center stretch of nine nucleotides was identified starting at 21 bp upstream of the *mazE* transcription start site (Fig. 1E). Using the same P_{mazE} fragment as in the EMSA experiments with MazE and MazF, we observed binding of purified SarA to this fragment, which could be competitively displaced by the addition of a 100-fold excess of unlabeled fragment, demonstrating specificity of binding (Fig. 6). Densitometric analysis of this EMSA revealed that the affinity (K_d) of SarA for P_{mazE} was 190 nM, a value in accordance with previous reports (39).

P_{mazE} is activated in response to various stress conditions. TA systems have been shown to be either up- or downregulated after exposure to heat or antibiotics (6, 13, 41). Previous studies have shown that a 48°C heat shock upregulates *sigB* transcription in *S. aureus* (43). Since *mazEF* is a TA system cotranscribed with *sigB*, we felt it necessary to better define the activity of P_{mazE} during various stresses. We first verified the effect of heat on *mazEF* transcription. As seen in Fig. 7, no elevation in either the 2.6-kb *rsbUVW-sigB* transcript from P_A or the 1.6-kb *rsbVW-sigB* from P_B was seen in Newman wild

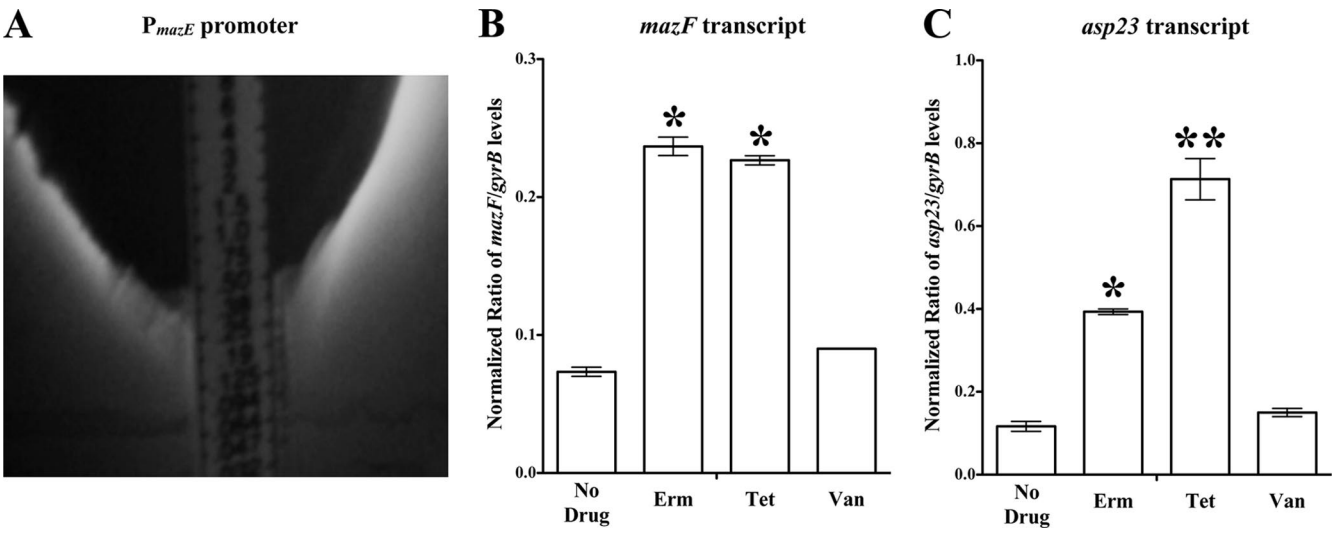

FIG. 8. (A) Antibiotic-induced fluorescence from Newman wild type containing a *mazEF* transcriptional fusion to gfp_{uvr} (pALC3961) grown on solid media. After 24 h of exposure to a tetracycline gradient created by an Etest strip, the fluorescence was recorded by using 518-nm filtered optics. (B and C) Relative quantification of *mazF* (B) and *asp23* (C) transcripts by real-time PCR of cDNA from Newman wild-type cells 1 to 2 mm proximal to the zone of clearing (i.e., the MIC) of tetracycline, erythromycin, or vancomycin disks. Newman wild type grown without exposure to antibiotics was used as a no-drug control. The data are presented as mean values for three experiments ± the standard deviation. *, $P < 0.0001$; **, $P \leq 0.0005$ (compared to the control [Student *t* test]).

type grown at 45°C, while transcription of the 3.7-kb transcript from P_{mazE} was increased under this condition (Fig. 7). A similar increase in transcription from P_{mazE} after heat shock was seen using a *mazF* probe (data not shown).

To clarify the effects of antibiotics on *mazEF* transcription, we first exposed Newman cells containing pALC3961 to an antibiotic gradient generated from an Etest strip. We observed that cells grown in the zone from one-quarter to the full MICs of tetracycline (125 to 500 ng/ml) became more fluorescent than untreated cells (Fig. 8A), indicating increased *mazEF* transcription in these regions. Other antibiotics (e.g., penicillin and linezolid) showed increases in similar ranges, while vancomycin produced no significant changes in fluorescence in these regions (data not shown). To quantitate these effects, RNA was purified from cells at this periphery and analyzed by real-time PCR. We observed that *mazEF* transcription was increased after exposure to tetracycline and erythromycin, but not vancomycin (Fig. 8B), a finding similar to what we observed in our fluorescence studies. Northern blot studies with a *mazF* probe also confirmed these findings for the 3.7-kb band (Fig. 9, top panel) and the 0.7-kb band (data not shown). Interestingly, a similar pattern was also noted for *asp23* transcription (Fig. 8C), again suggesting a role for P_{mazE} in controlling overall σ^B activity. Based on these results, we concluded that not all antibiotics affect P_{mazE}, but those that do, do so strongly, and that this activity can be triggered from a full MIC down to one-quarter of the MIC. Furthermore, these data indicated that *mazEF* transcription can remain elevated for over 24 h in cells grown on solid agar in the presence of subinhibitory concentrations of antibiotics.

Antibiotics stimulate transcription of other TA systems in *S. aureus*. The induction of *mazEF* transcription upon exposure to some antibiotics made us curious as to whether *axe1*/*txe1* and *axe2*/*txe2* in *S. aureus* were similarly affected. Accordingly, we extracted RNA from *S. aureus* Newman cells exposed to subinhibitory concentrations of tetracycline (78 ng/ml), erythromycin (312 ng/ml), and vancomycin (1 μg/ml) and performed Northern blot analysis using probes to *txe1* and *txe2*. Under

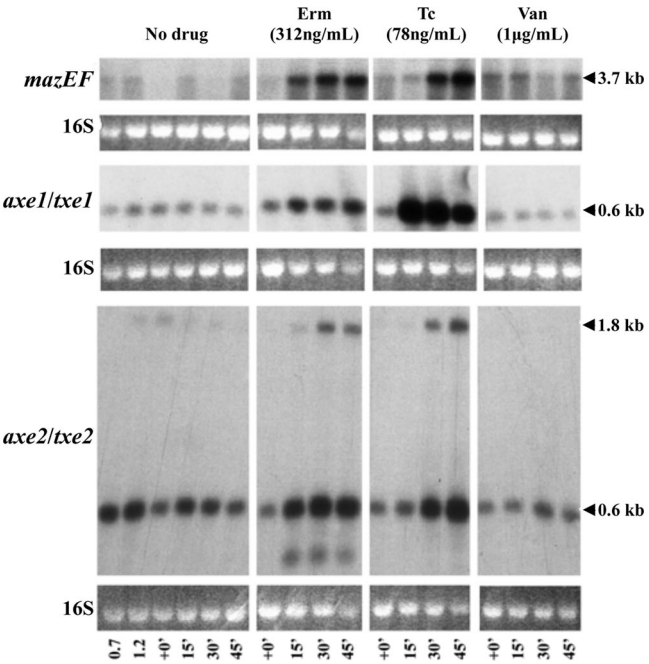

FIG. 9. Northern blot analyses of *mazEF*, *axe1*/*txe1*, and *axe2*/*txe2* mutants were performed on RNA purified from Newman cells exposed to erythromycin (312 ng/ml), tetracycline (78 ng/ml), or vancomycin (1 μg/ml). The sizes of the relevant bands are indicated on the right, and the staining patterns of 16S rRNA with ethidium bromide for each gel are shown below.

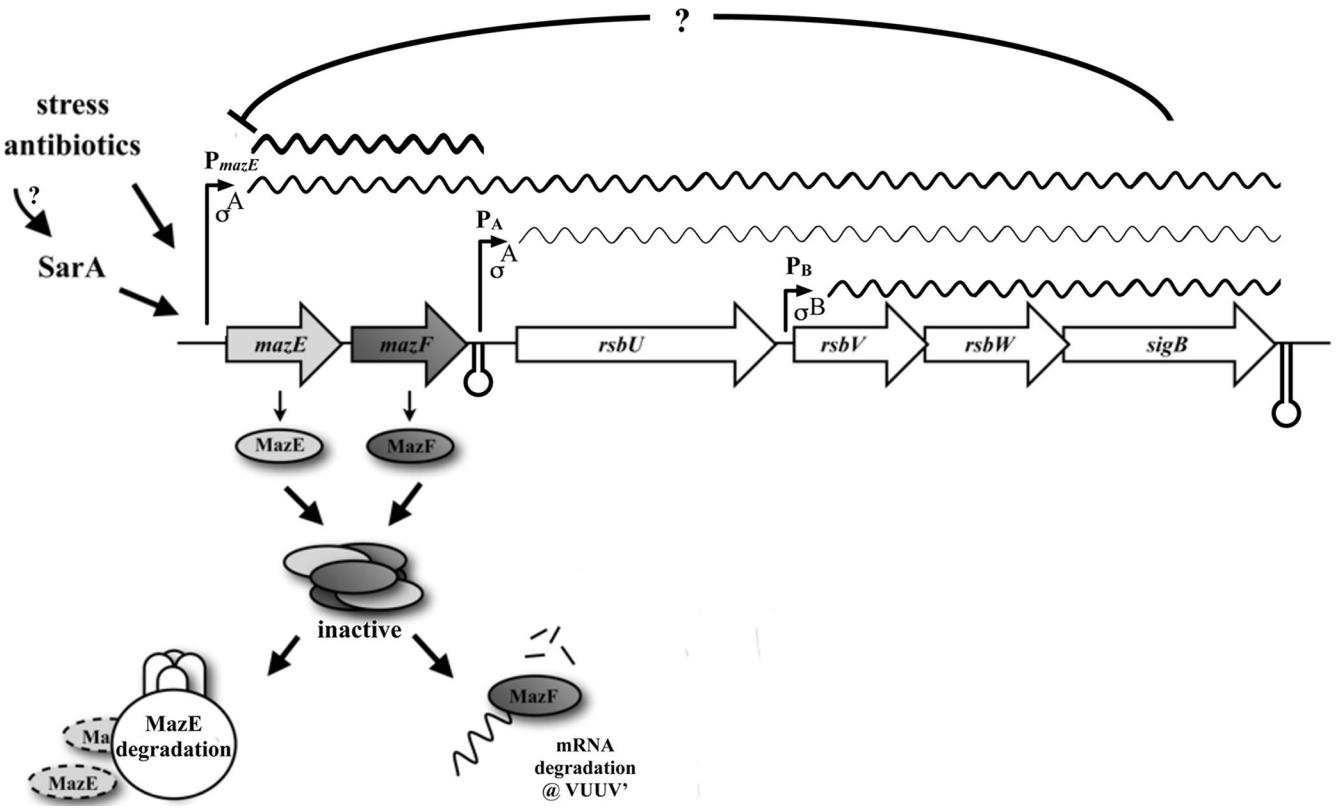

FIG. 10. Proposed model for *mazEF* regulation in *S. aureus*. Transcription initiated from P_{mazE} combined with a weak *rho*-independent terminator downstream of *mazF* creates both the 0.7-kb *mazEF* transcript and a 3.7-kb *mazEF-rsbUVW-sigB* transcript. This latter transcript is required for full σ^B activity and contributes significantly to *rsbU*-related transcripts, since the activity of the P_A promoter is weak. Transcription from P_{mazE} is stimulated by environmental and antibiotic stress, which may be mediated by the direct binding of SarA at the −35 site of the promoter. Transcription of the 0.7- and 3.7-kb mRNAs is also negatively regulated by *sigB*, likely through an intermediary. It is possible that this establishes a negative-feedback loop wherein *sigB* represses P_{mazE}. The *mazEF* translational products ultimately produce a TA system in which the antitoxin MazE binds and inactivates MazF in a higher-order stoichiometry. After proteolytic degradation of MazE by ATP-dependent proteases, MazF of *S. aureus* degrades mRNA at the VUUV′ sequence in susceptible mRNA (17).

noninducing conditions, both *axe1*/*txe1* and *axe2*/*txe2* were transcribed as ~0.6-kb mRNAs, corresponding to the genes in each system (Fig. 9). In addition, *axe2*/*txe2* was also part of an 1.8-kb transcript, likely encompassing the neighboring SA2244, a 1,077-bp gene that encodes a putative endo-1,4-β-glucanase. After antibiotic challenge, we also observed a transcriptional pattern similar to that of *mazEF* (Fig. 9). More specifically, both *axe1*/*txe1* and *axe2*/*txe2* transcripts were upregulated after exposure to erythromycin and tetracycline, but not with vancomycin. Furthermore, transcription of all of these systems reached their maximum within 30 to 45 min of exposure to either erythromycin or tetracycline. Together, these results indicate that all known TA systems in *S. aureus* are rapidly activated upon exposure to subinhibitory concentrations of selective antibiotics and likely remain so for the duration of the exposure.

DISCUSSION

In this study, we demonstrated that the σ^A-dependent promoter P_{mazE} contributes to σ^B activity by producing a 3.7-kb *mazEF-rsbUVW-sigB* mRNA. We observed this promoter to be inducible by heat shock and by exposure to subinhibitory concentrations of certain antibiotics, which boost *sigB* transcription and σ^B activity under these conditions. In addition, a small 0.7-kb *mazEF* transcript was also observed, likely due to transcriptional termination from a weak *rho*-independent terminator between *mazF* and *rsbU* (14). Interestingly, other species with a similar *sigB* operon structure (i.e., *B. subtilis*, *Listeria* spp., and other *Staphylococcus* spp.) all had much stronger transcriptional terminators in this location (14), which presumably prevent readthrough by RNA polymerase. This finding suggests that cotranscription of *mazEF* with *rsbUVW-sigB*, and hence P_{mazE}'s influence on σ^B activity, may be limited solely to *S. aureus*. Furthermore, as *sigB* in *S. aureus* also controls selective aspects of virulence gene expression in addition to stress response (5), we speculate that the linking of this promoter to the *sigB* operon in *S. aureus* may have enhanced control of this larger regulon.

In the course of these investigations, we were surprised to find that P_{mazE} was not regulated by its own gene products, in contrast to all other TA systems examined thus far (18). Instead, it appeared to be negatively regulated by *sigB*, the last gene in the 3.7-kb *mazEF-rsbUVW-sigB* transcript. In addition to *sigB* repressing *mazEF*, this may also function as a feedback loop to return elevated *sigB* transcription (e.g., after activation

of the feed-forward σ^B-dependent P_B promoter) to basal levels. However, direct repression of P_{mazE} by *sigB* is unlikely since P_{mazE} is a σ^A-dependent promoter. One possible mechanism for this repression could be via a *sigB*-regulated repressor. Two such transcriptional repressors in *S. aureus*, *yabJ* and *spoVG* (5), were examined for such a role, but no differences in *mazEF* transcription were observed in either the single or double deletion mutant strains of these genes (data not shown). Another possible mechanism might involve sigma factor competition (32), where the absence of σ^B in a Δ*sigB* strain could permit σ^A increased access to RNA polymerase, thus increasing transcription from σ^A-dependent promoters. Such competition is seen in *B. subtilis* after exposure to environmental stress (40), and we are currently examining *S. aureus* for similar regulation.

P_{mazE} was also shown to be positively and directly regulated by SarA, a winged-helix transcriptional regulator of virulence gene expression in *S. aureus* (11, 15). Based on previous promoter binding studies (12, 31), SarA likely binds to an inverted repeat that overlaps the −35 promoter region of P_{mazE}. While occlusion of this −35 box by SarA might be initially thought to reduce σ^A's ability to initiate transcription at this promoter, the presence of a 5′-TG-3′ extended −10 motif at position −15/−16 from the *mazEF* transcription start site (23) suggests this may not be the case. Such a motif has been shown to be sufficient in compensating for the absence of a −35 region box of a σ^A promoter (7), and this leniency in promoter requirement may enable SarA to act on RNA polymerase as a transcriptional activator. Furthermore, SarA was shown not to bind to either the P_A or P_B promoters in the *sigB* operon (data not shown), making P_{mazE} the only region where *sarA* regulation could affect *sigB* transcription.

To date, TA transcriptional regulation has been thought to be mediated solely via autorepression. However, our findings that *sarA* and *sigB* regulate the *mazEF* system in *S. aureus* indicate that diverse regulatory mechanisms may yet exist for TA systems of other species. Such pathways may finally explain how TA promoters can be either activated (6, 13) or repressed (1, 41) following environmental, nutritional, or antibiotic challenges. Our data here show a similar regulatory flexibility, since *mazEF* levels were likely to be lower in the nutritionally depleted conditions of late stationary cultures ($t = 16$ h) but were increased after heat shock or exposure to antibiotics such as tetracycline and erythromycin. Interestingly, this induction was maintained for over 24 h, indicating that these cells remained transcriptionally active even while producing large amounts of TA transcripts. A further point of interest was that certain antibiotics, such as vancomycin, failed to induce TA expression, indicating that there may be yet further criteria for TA activation.

In summary, the σ^A-dependent P_{mazE} promoter was revealed to be essential for full σ^B activity due to its transcriptional linkage with the downstream *sigB* operon via readthrough of a weak downstream *rho*-independent terminator (Fig. 10). P_{mazE} drives the 3.7-kb transcript, contributing significantly to the transcription of *rsbU* and *sigB* since the promoter upstream of *rsbU* is relatively weak. P_{mazE} was also found to be positively regulated by SarA, which likely binds at a site overlapping the −35 box. In contrast to all other TA systems examined, autoregulation of P_{mazE} was not found to occur, although transcriptional repression by *sigB* downstream may perform a similar role. Furthermore, since this promoter was strongly active in the presence of certain antibiotics or heat shock, but inactive during late stationary phase, divergent roles for TA systems may exist during various stress responses.

ACKNOWLEDGMENTS

We thank A. Manna for assistance with the EMSA, primer extension, and Northern blotting and D. Reyes and S. Tamber for editorial comments.

This study was supported in part by AI56114 and AI37142 from the National Institutes of Health (to A.L.C.).

REFERENCES

1. **Aizenman, E., H. Engelberg-Kulka, and G. Glaser.** 1996. An *Escherichia coli* chromosomal "addiction module" regulated by guanosine 3′,5′-bispyrophosphate: a model for programmed bacterial cell death. Proc. Natl. Acad. Sci. USA **93:**6059–6063.
2. **Arnaud, M., A. Chastanet, and M. Debarbouille.** 2004. New vector for efficient allelic replacement in naturally non-transformable, low-GC-content, gram-positive bacteria. Appl. Environ. Microbiol. **70:**6887–6891.
3. **Bae, T., A. K. Banger, A. Wallace, E. M. Glass, F. Aslund, O. Schneewind, and D. M. Missiakas.** 2004. *Staphylococcus aureus* virulence genes identified by *bursa aurealis* mutagenesis and nematode killing. Proc. Natl. Acad. Sci. USA **101:**12312–12317.
4. **Bayer, M. G., J. H. Heinrichs, and A. L. Cheung.** 1996. The molecular architecture of the *sar* locus in *Staphylococcus aureus*. J. Bacteriol. **178:**4563–4570.
5. **Bischoff, M., P. Dunman, J. Kormanec, D. Macapagal, E. Murphy, W. Mounts, B. Berger-Bachi, and S. Projan.** 2004. Microarray-based analysis of the *Staphylococcus aureus* σ^B regulon. J. Bacteriol. **186:**4085–4099.
6. **Budde, P. P., B. M. Davis, J. Yuan, and M. K. Waldor.** 2007. Characterization of a *higBA* toxin-antitoxin locus in *Vibrio cholerae*. J. Bacteriol. **189:**491–500.
7. **Camacho, A., and M. Salas.** 1999. Effect of mutations in the "extended −10" motif of three *Bacillus subtilis* σ^A-RNA polymerase-dependent promoters. J. Mol. Biol. **286:**683–693.
8. **Cheung, A. L., K. J. Eberhardt, and V. A. Fischetti.** 1994. A method to isolate RNA from gram-positive bacteria and mycobacteria. Anal. Biochem. **222:** 511–514.
9. **Cheung, A. L., and A. C. Manna.** 2005. Role of the distal *sarA* promoters in SarA expression in *Staphylococcus aureus*. Infect. Immun. **73:**4391–4394.
10. **Cheung, A. L., C. C. Nast, and A. S. Bayer.** 1998. Selective activation of *sar* promoters with the use of green fluorescent protein transcriptional fusions as the detection system in the rabbit endocarditis model. Infect. Immun. **66:** 5988–5993.
11. **Cheung, A. L., K. A. Nishina, M. P. Trotonda, and S. Tamber.** 2008. The SarA protein family of *Staphylococcus aureus*. Int. J. Biochem. Cell Biol. **40:**355–361.
12. **Chien, Y.-t., A. C. Manna, S. J. Projan, and A. L. Cheung.** 1999. SarA, a global regulator of virulence determinants in *Staphylococcus aureus*, binds to a conserved motif essential for *sar*-dependent gene regulation. J. Biol. Chem. **274:**37169–37176.
13. **Christensen, S. K., M. Mikkelsen, K. Pedersen, and K. Gerdes.** 2001. RelE, a global inhibitor of translation, is activated during nutritional stress. Proc. Natl. Acad. Sci. USA **98:**14328–14333.
14. **de Hoon, M. J., Y. Makita, K. Nakai, and S. Miyano.** 2005. Prediction of transcriptional terminators in *Bacillus subtilis* and related species. PLoS Comput. Biol. **1:**e25.
15. **Dunman, P. M., E. Murphy, S. Haney, D. Palacios, G. Tucker-Kellogg, S. Wu, E. L. Brown, R. J. Zagursky, D. Shlaes, and S. J. Projan.** 2001. Transcription profiling-based identification of *Staphylococcus aureus* genes regulated by the *agr* and/or *sarA* loci. J. Bacteriol. **183:**7341–7353.
16. **Duthie, E. S., and L. L. Lorenz.** 1952. Staphylococcal coagulase; mode of action and antigenicity. J. Gen. Microbiol. **6:**95–107.
17. **Fu, Z., N. P. Donegan, G. Memmi, and A. L. Cheung.** 2007. Characterization of $MazF_{sa}$, an endoribonuclease from *Staphylococcus aureus*. J. Bacteriol. **189:**8871–8879.
18. **Gerdes, K., S. K. Christensen, and A. Lobner-Olesen.** 2005. Prokaryotic toxin-antitoxin stress response loci. Nat. Rev. Microbiol. **3:**371–382.
19. **Gertz, S., S. Engelmann, R. Schmid, K. Ohlsen, J. Hacker, and M. Hecker.** 1999. Regulation of σ^B-dependent transcription of *sigB* and *asp23* in two different *Staphylococcus aureus* strains. Mol. Gen. Genet. **261:**558–566.
20. **Gotfredsen, M., and K. Gerdes.** 1998. The *Escherichia coli relBE* genes belong to a new toxin-antitoxin gene family. Mol. Microbiol. **29:**1065–1076.
21. **Grady, R., and F. Hayes.** 2003. Axe-Txe, a broad-spectrum proteic toxin-antitoxin system specified by a multidrug-resistant, clinical isolate of *Enterococcus faecium*. Mol. Microbiol. **47:**1419–1432.

22. **Hecker, M., J. Pane-Farre, and U. Volker.** 2007. σ^B-dependent general stress response in *Bacillus subtilis* and related gram-positive bacteria. Annu. Rev. Microbiol. **61:**215–236.
23. **Helmann, J. D.** 1995. Compilation and analysis of *Bacillus subtilis* σ^A-dependent promoter sequences: evidence for extended contact between RNA polymerase and upstream promoter DNA. Nucleic Acids Res. **23:**2351–2360.
24. **Igoshin, O. A., M. S. Brody, C. W. Price, and M. A. Savageau.** 2007. Distinctive topologies of partner-switching signaling networks correlate with their physiological roles. J. Mol. Biol. **369:**1333–1352.
25. **Katzif, S., E.-H. Lee, A. B. Law, Y.-L. Tzeng, and W. M. Shafer.** 2005. CspA regulates pigment production in *Staphylococcus aureus* through a σ^B-dependent mechanism. J. Bacteriol. **187:**8181–8184.
26. **King, M. D., B. J. Humphrey, Y. F. Wang, E. V. Kourbatova, S. M. Ray, and H. M. Blumberg.** 2006. Emergence of community-acquired methicillin-resistant *Staphylococcus aureus* USA 300 clone as the predominant cause of skin and soft-tissue infections. Ann. Intern. Med. **144:**309–317.
27. **Kluytmans, J., A. van Belkum, and H. Verbrugh.** 1997. Nasal carriage of *Staphylococcus aureus*: epidemiology, underlying mechanisms, and associated risks. Clin. Microbiol. Rev. **10:**505–520.
28. **Kreiswirth, B. N., S. Lofdahl, M. J. Betley, M. O'Reilly, P. M. Schlievert, M. S. Bergdoll, and R. P. Novick.** 1983. The toxic shock syndrome exotoxin structural gene is not detectably transmitted by a prophage. Nature **305:**709–712.
29. **Kullik, I., R. Jenni, and B. Berger-Bachi.** 1998. Sequence of the putative alanine racemase operon in *Staphylococcus aureus*: insertional interruption of this operon reduces D-alanine substitution of lipoteichoic acid and autolysis. Gene **219:**9–17.
30. **Liu, G. Y., A. Essex, J. T. Buchanan, V. Datta, H. M. Hoffman, J. F. Bastian, J. Fierer, and V. Nizet.** 2005. *Staphylococcus aureus* golden pigment impairs neutrophil killing and promotes virulence through its antioxidant activity. J. Exp. Med. **202:**209–215.
31. **Liu, Y., A. C. Manna, C.-H. Pan, I. A. Kriksunov, D. J. Thiel, A. L. Cheung, and G. Zhang.** 2006. Structural and function analyses of the global regulatory protein SarA from *Staphylococcus aureus*. Proc. Natl. Acad. Sci. USA **103:**2392–2397.
32. **Maeda, H., N. Fujita, and A. Ishihama.** 2000. Competition among seven *Escherichia coli* σ subunits: relative binding affinities to the core RNA polymerase. Nucleic Acids Res. **28:**3497–3503.
33. **Magnuson, R. D.** 2007. Hypothetical functions of toxin-antitoxin systems. J. Bacteriol. **189:**6089–6092.
34. **Meehl, M., S. Herbert, F. Gotz, and A. Cheung.** 2007. Interaction of the GraRS two-component system with the VraFG ABC transporter to support vancomycin-intermediate resistance in *Staphylococcus aureus*. Antimicrob. Agents Chemother. **51:**2679–2689.
35. **Meier, S., C. Goerke, C. Wolz, K. Seidl, D. Homerova, B. Schulthess, J. Kormanec, B. Berger-Bachi, and M. Bischoff.** 2007. σ^B and the σ^B-dependent *arlRS* and *yabJ-spoVG* loci affect capsule formation in *Staphylococcus aureus*. Infect. Immun. **75:**4562–4571.
36. **Palma, M., A. Bayer, L. I. Kupferwasser, T. Joska, M. R. Yeaman, and A. Cheung.** 2006. Salicylic acid activates σ^B by *rsbU*-dependent and -independent mechanisms. J. Bacteriol. **188:**5896–5903.
37. **Palma, M., and A. L. Cheung.** 2001. σ^B Activity in *Staphylococcus aureus* is controlled by RsbU and an additional factor(s) during bacterial growth. Infect. Immun. **69:**7858–7865.
38. **Pandey, D. P., and K. Gerdes.** 2005. Toxin-antitoxin loci are highly abundant in free-living but lost from host-associated prokaryotes. Nucleic Acids Res. **33:**966–976.
39. **Rechtin, T. M., A. F. Gillaspy, M. A. Schumacher, R. G. Brennan, M. S. Smeltzer, and B. K. Hurlburt.** 1999. Characterization of the SarA virulence gene regulator of *Staphylococcus aureus*. Mol. Microbiol. **33:**307–316.
40. **Rollenhagen, C., H. Antelmann, J. Kirstein, O. Delumeau, M. Hecker, and M. D. Yudkin.** 2003. Binding of σ^A and σ^B to core RNA polymerase after environmental stress in *Bacillus subtilis*. J. Bacteriol. **185:**35–40.
41. **Sat, B., R. Hazan, T. Fisher, H. Khaner, G. Glaser, and H. Engelberg-Kulka.** 2001. Programmed cell death in *Escherichia coli*: some antibiotics can trigger *mazEF* lethality. J. Bacteriol. **183:**2041–2045.
42. **Schenk, S., and R. A. Laddaga.** 1992. Improved method for electroporation of *Staphylococcus aureus*. FEMS Microbiol. Lett. **73:**133–138.
43. **Senn, M. M., P. Giachino, D. Homerova, A. Steinhuber, J. Strassner, J. Kormanec, U. Fluckiger, B. Berger-Bachi, and M. Bischoff.** 2005. Molecular analysis and organization of the σ^B operon in *Staphylococcus aureus*. J. Bacteriol. **187:**8006–8019.
44. **Shafer, W. M., and J. J. Iandolo.** 1979. Genetics of staphylococcal enterotoxin B in methicillin-resistant isolates of *Staphylococcus aureus*. Infect. Immun. **25:**902–911.
45. **Solberg, C. O.** 2000. Spread of *Staphylococcus aureus* in hospitals: causes and prevention. Scand. J. Infect. Dis. **32:**587–595.
46. **Taylor, M. D., and L. M. Napolitano.** 2004. Methicillin-resistant *Staphylococcus aureus* infections in vascular surgery: increasing prevalence. Surg. Infect. **5:**180–187.
47. **Wiedmann, M., T. J. Arvik, R. J. Hurley, and K. J. Boor.** 1998. General stress transcription factor σ^B and its role in acid tolerance and virulence of *Listeria monocytogenes*. J. Bacteriol. **180:**3650–3656.
48. **Zhang, J., Y. Zhang, and M. Inouye.** 2003. Characterization of the interactions within the *mazEF* addiction module of *Escherichia coli*. J. Biol. Chem. **278:**32300–32306.